

Article

Numerical Simulation on the Smoke Prevention Performance of Air Curtains in an Island-Type Subway Station

Xu Yan ¹, Hongyun Yang ², Huiqiang Mo ³, Ye Xie ², Zhongfu Jin ² and Yang Zhou ^{1,*}¹ School of Civil Engineering, Central South University, Changsha 410075, China² Intelligent Transportation Institute of Zhejiang Communication Investment Group Co., Ltd., Hangzhou 310020, China³ Zhejiang Rail Transit Operation Management Group Co., Ltd., Hangzhou 310020, China

* Correspondence: zyzhou@csu.edu.cn

Abstract: Subway fires are a major threat to the safe and smooth operation of subway stations. In this paper, an island-type subway station was taken as an example to conduct a series of numerical simulations using Fire Dynamics Simulator (FDS). The temperature, visibility, and CO concentration in the subway station were analysed under different thicknesses and jet velocities of the air curtains. The smoke-prevention performance of the air curtains in the subway station was investigated. As the thickness and jet velocity increase, the flame tilts significantly, which greatly hinders the spread of smoke toward the stairs. The smoke temperature and CO concentration on the left side of the air curtains gradually decrease, while the visibility increases significantly. For a 3 MW fire scenario, to satisfy the evaluation criteria, the results show that the thickness of the air curtains needs to be at least 0.3 m, and the jet velocity needs to be at least 2 m/s. The sealing effectiveness ($E_{sealing}$) tends to increase and then remains constant with increasing momentum, and the maximum is obtained when the momentum of the air curtains (I_a) is 12.5 kg·m/s². Meanwhile, it is found that an energy-saving efficiency of 85.2% can be achieved by replacing positive pressure ventilation with air curtains. The results of this work can provide a significant reference for the design of smoke protection in subway stations.



Citation: Yan, X.; Yang, H.; Mo, H.; Xie, Y.; Jin, Z.; Zhou, Y. Numerical Simulation on the Smoke Prevention Performance of Air Curtains in an Island-Type Subway Station. *Fire* **2023**, *6*, 177. <https://doi.org/10.3390/fire6050177>

Academic Editors: Yanming Ding, Kazui Fukumoto and Jiaqing Zhang

Received: 16 March 2023

Revised: 4 April 2023

Accepted: 5 April 2023

Published: 26 April 2023

Corrected: 29 September 2023

Keywords: air curtain; smoke spread; subway station; momentum

1. Introduction

With the further advancement of the urbanization process and the increasing trend of population concentration in large cities, the original public transportation cannot meet the needs of urban development. The subway has gradually become the preferred means of transportation in large cities, due to its high passenger capacity, high speed, and reliability [1]. According to statistics, a total of 45 cities in China have opened and operated 244 urban rail transit lines by the end of 2021. Once a safety accident occurs, such a huge subway system will become very dangerous. One of the main threats facing subway stations is fire [2,3]. Passengers will have difficulty evacuating in emergencies since the platform floor and the station hall floor are only connected by a few stairs. Additionally, the spreading direction of the smoke is the same as the direction of the evacuation of the passengers, which will seriously threaten the safety of the passengers. For example, the fire at London's King's Cross Underground Station in 1987 killed 31 people [4]. The Jungangno subway station was set on fire due to arson in Daegu, South Korea in 2003, resulting in 192 deaths [5]. The heat and smoke produced by fire are the main causes of death in fire accidents [6]. To ensure the evacuation of people, China's "Code for safety evacuation of metro [7]" stipulates that a downward airflow of 1.5 m/s should be formed at the opening of the evacuation stairs and escalator to block the smoke from spreading from the platform floor to the station hall floor. However, this downward airflow of 1.5 m/s is not easy to



Copyright: © 2023 by the authors. Licensee MDPI, Basel, Switzerland. This article is an open access article distributed under the terms and conditions of the Creative Commons Attribution (CC BY) license (<https://creativecommons.org/licenses/by/4.0/>).

achieve, and there are some locations where it is difficult to block the smoke, due to the limits of equipment, site, etc. [8]. The performance of positive pressure ventilation alone is not ideal. Therefore, this paper aims to find an effective device to block smoke to ensure the safety of passengers during evacuation in the event of a fire.

The air curtain is a device used to separate different environmental areas. For example, it can effectively isolate the mass and heat transfer between the two separated areas, and it is particularly needed where substantial barriers are not allowed [9]. In recent years, due to the advantages of air curtains over traditional smoke-prevention methods, the application of air curtains in the field of smoke prevention has attracted widespread attention. Yang et al. adopted three strategies of mechanical ventilation to study the control effect of different fire source positions on smoke, and concluded that air curtains have many advantages in smoke-prevention performance [10]. Luo N et al. conducted experiments and numerical simulations to study the efficacy of air curtains in confining fire-induced smoke transportation in a high-rise building [11]. Razeghi et al. studied the smoke-prevention performance of an air curtain under different jet velocities and angles as well as smoke exhaust velocity, and gave the appropriate jet velocity and angle for 200 kW and 500 kW fires in the room [12]. Gupta et al. studied the effect of the jet angle of the air curtain and the smoke exhaust velocity on the smoke-prevention performance of a double-layer air curtain through experiments [13]. Zhou et al. studied the influence of the jet direction of a double-layer air curtain on the smoke-prevention performance, and finally determined the appropriate jet direction through Computational Fluid Dynamics (CFD) and Fire Dynamics Simulator (FDS) simulation [14]. Due to the excellent performance of the air curtain in smoke prevention, many scholars have begun to try to apply the air curtain to tunnels. Hu et al. studied the blocking effect of air curtains on smoke and carbon monoxide in the tunnel through experiments and simulations [15]. Jung et al. used CFD to study the smoke-prevention performance of air curtains under different jet angles and jet velocities in the tunnel, and the results showed that a jet angle of 20° is the most appropriate, and the jet velocity needs to be determined according to the static pressure difference at the entrance and exit of the tunnel [16]. Jin et al. used FDS to study the smoke-prevention performance of the air curtain under different jet angles and jet velocities in the tunnel from the three dimensions of smoke temperature, visibility, and CO concentration, and the results indicated that the best smoke-prevention performance can be achieved under the conditions of 20° and 10 m/s [17]. Chen et al. combined theoretical analysis and simulation to study the temperature change and the longitudinal variation law of heat decay in the tunnel under the conditions of natural ventilation and air curtains, and the results showed that the air curtain can effectively isolate the diffusion of heat flow [18]. Gao et al. conducted full-scale experiments in the tunnel to determine the appropriate air curtain jet velocity to prevent the spread of smoke, and found the relationship between the design parameters of air curtains (jet velocity, jet angle, thickness) and heat release rate through Fluent [19].

However, the existing research on air curtains was mainly aimed at tunnels, and relatively few scholars have applied air curtains to subway stations. This paper studied the smoke-prevention performance of air curtains with different jet velocities and thicknesses, under the condition of positive pressure ventilation, to verify its practicability in subway stations. Considering the repeatability of the positive pressure ventilation with air curtains in terms of the air supply and the lower air supply volume of air curtains, the smoke-prevention performance of air curtains was studied to determine whether the positive pressure ventilation can be replaced by air curtains to achieve the efficiency of energy saving.

2. FDS Model

2.1. Numerical Modelling

Fire Dynamics Simulator (FDS) is a fire dynamics simulation tool developed by NIST (National Institute of Standards and Technology), a computational fluid dynamics program.

A common island-type subway station was constructed in FDS, and the internal structure is shown in Figure 1. The specific parameters of the subway station are shown in Table 1. Baffles were also set on both sides of the stairs. However, baffles were not presented in Figure 1 for the convenience of observation. Since the bottleneck location during evacuation of a subway station is the stairway entrance [20], the fire source was located 3 m to the right of the stairs, which is in the middle of the subway platform, and the size was selected as $1\text{ m} \times 1\text{ m}$. The visibility measuring points interval was $1.8\text{ m} \times 1.8\text{ m}$. The visibility measuring points, the temperature measuring point, and the CO measuring point were set at a height of 2 m (the height of the human eyes). 50 smoke vents ($1.5\text{ m} \times 0.75\text{ m}$) were installed on the platform ceiling. To ensure that the positive pressure air supply works, the volume of smoke exhausted needs to be equal to the volume of air supplied to keep the pressure in the station balanced. Meanwhile, the Code for safety evacuation of metro stipulates that when a fire occurs in the station hall or platform, the volume of smoke exhausted at the underground station platform and station hall should be calculated according to the construction area of the smoke prevention zone at $1\text{ m}^3/(\text{m}^2 \cdot \text{min})$. The specific volume of smoke exhausted for each working condition will be given in Section 2.3. Fans were installed at the station hall to provide positive pressure ventilation at the speed of 1.5 m/s (this is also verified by the data in the results).

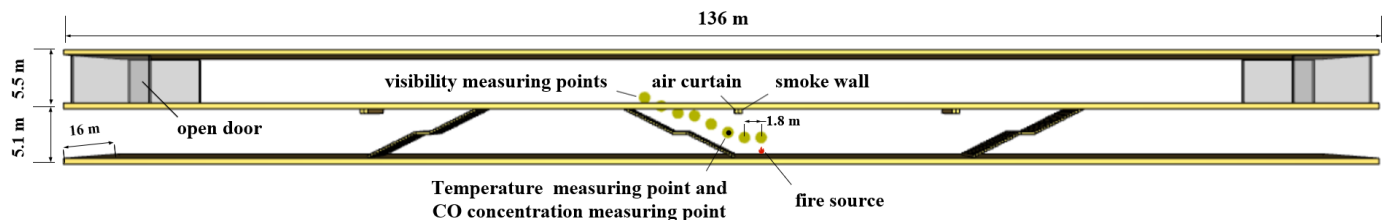


Figure 1. Model of the subway station.

Table 1. Dimensions of the subway station.

Dimension		Value (m)
Station hall/platform	Length	136
	Width	16
	Height	5.1/5.5
Open doors	Width	8
	Height	5.5
Stairs	Length	11.4
	Width	8
	Height	5.1
Smoke walls	Length	8
	Width	0.4
	Height	0.5
Air curtains	Length	8
	Thickness	0.2/0.3/0.4
	Height	0.5

2.2. Grid Independence Study

The choice of grid size will be related to the accuracy of the simulation results and the length of the calculation time. Grids that are too large or too small are unacceptable. The grid selection method in the FDS user's guide is accepted by most scholars [8,21]. The

method uses a dimensionless constant $D^*/\delta x$ to calculate the grid size, where D^* is the characteristic fire diameter and δx is the selected grid size. D^* is defined by Equation (1):

$$D^* = \left(\frac{\dot{Q}}{\rho_{\infty} c_p T_{\infty} \sqrt{g}} \right)^{\frac{2}{5}} \quad (1)$$

where, \dot{Q} is the heat release rate of the fire source, kW; ρ_{∞} is the density of the air, kg/m³; c_p is the specific heat capacity at constant pressure, J/(kg·K); T_{∞} is the initial ambient temperature, K; g is the gravitational acceleration, m/s².

Based on Equation (1), the calculated value of D^* is 1.45 in this paper. The FDS user's guide suggested that the ratio of $D^*/\delta x$ should be from 4 to 16. It means the range of δx is from 0.09 m to 0.36 m. Therefore, 0.1 m, 0.2 m, and 0.3 m grids were selected for grid sensitivity analysis. Figure 2 shows the smoke temperature changes at 0.2 m below the ceiling which is 7 m to the right of the fire source at the platform under different grids. The temperature when the grid is 0.3 m is lower than in other grids. Considering the calculation time and the performance of the computer CPU, the final grid was selected as 0.2 m. Thus, the grid of the areas around the fire source and stairs was selected as 0.2 m, and the grid of other areas was selected as 0.6 m.

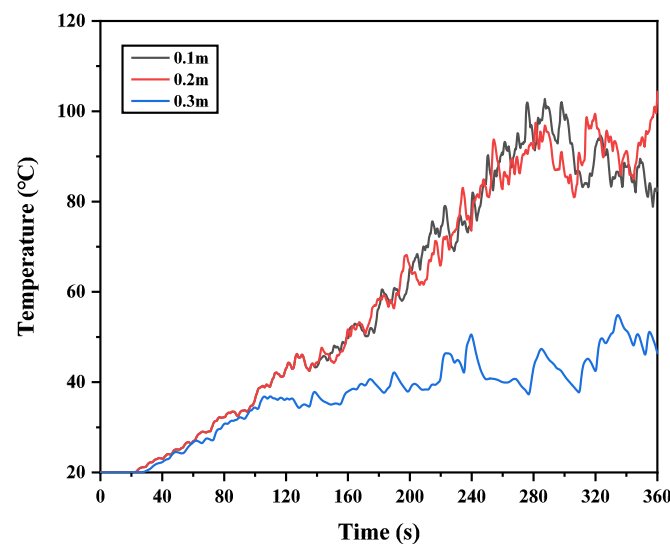


Figure 2. Temperature changes under different grids.

2.3. Working Conditions and Boundary Conditions

The jet velocity and thickness are crucial design parameters in directly affecting the smoke-prevention performance of an air curtain. The jet velocity range was selected as 0~3 m/s, and the thickness was selected as 0.2~0.4 m. The designed working conditions for the simulation are shown in Table 2. The ambient temperature was 293.15 K. The pressure inside the subway station was 101.3 kPa. Hansell has calculated the fire heat release rate in public places, and posits the idea that the fire scale is mostly in the range of 2~2.5 MW [22]. In this paper, to allow redundancy for engineering design, a fire source with a power of 3 MW in a rapid growth mode, which means 20% engineering redundancy for the upper limit of heat release rate, was selected for research. The fire source power reaches its peak value at 252 s. According to the US standard NFPA130 for fixed rail transportation and passenger car systems, safe evacuation time needs to be within 6 min [23]. Therefore, the simulation time was 360 s.

Table 2. Working conditions.

NO.	v (m/s)	d (m)	Positive Pressure Ventilation	The Volume of Smoke Exhausted (m^3/s)
1	/	/	✓	82.8
2–19	0.5	0.2/0.3/0.4	✓	85.2/88.8/93.6
	1		✓	87.6/90/92.4
	1.5		✓	90/93.6/97.2
	2		✓	92.4/97.2/102
	2.5		✓	94.8/100.8/106.8
	3		✓	97.2/104.4/116.2
21–22	3.5/4	0.2	✓	99.6/102
23	3.5	0.3	✓	108
24	2	0.3	×	36.3

2.4. Evaluation Criteria

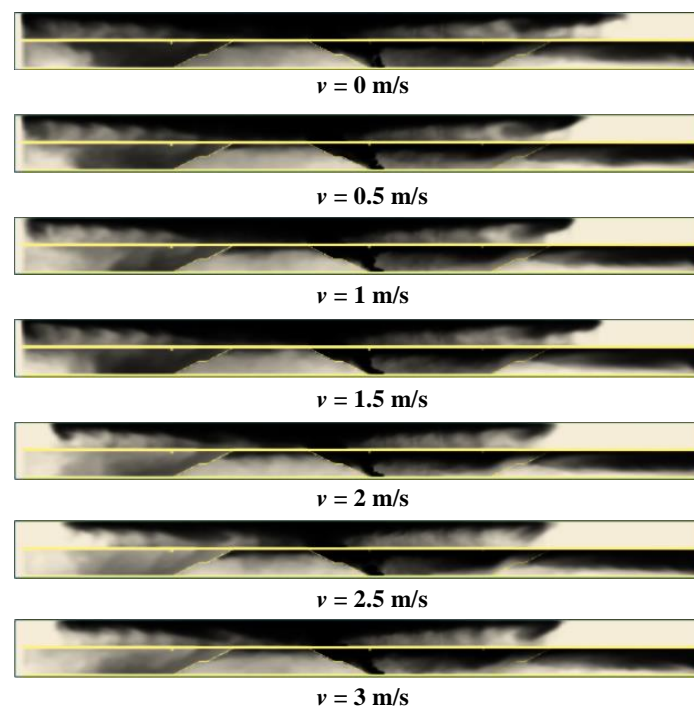
Emergency plans play an important role in the development of emergency management systems [24,25]. And among them, safety evacuation is of great significance to ensure that personnel escape from dangerous situations smoothly during emergencies [26]. Evaluation criteria need to be given to be quantified to measure the smoke-prevention performance of air curtains during the evacuation. Referring to some scholars and literature, this paper decided to use temperature, visibility, and CO concentration as evaluation criteria [27,28]. Conditions are considered safe only when the temperature is below 60 °C, the visibility is above 10 m, and the CO concentration is below 500 ppm [29,30].

3. Results and Discussion

3.1. Influence of the Air Curtain

3.1.1. Smoke Spread Process

Figures 3–5, respectively, show the smoke spread at different jet velocities at 360 s when the thickness of the air curtains is 0.2 m, 0.3 m, and 0.4 m.

**Figure 3.** Smoke spread at 360 s ($d = 0.2$ m).

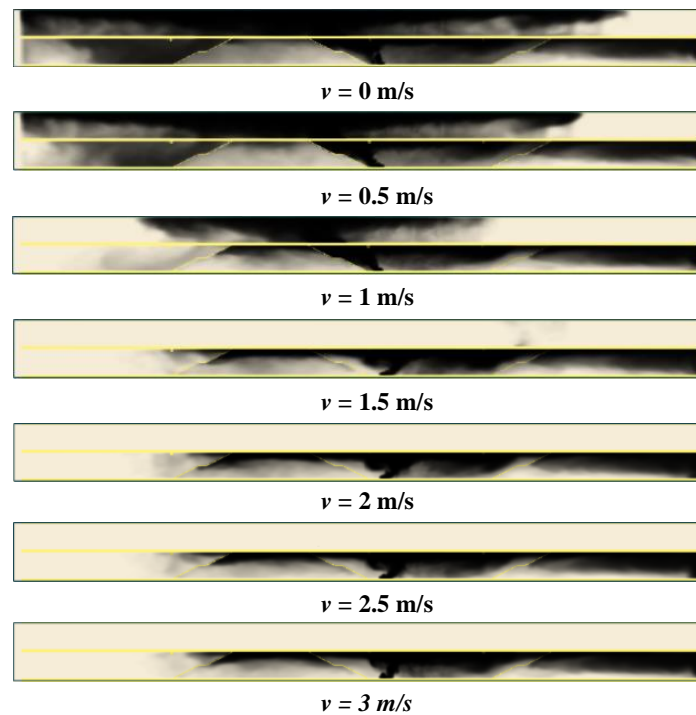


Figure 4. Smoke spread at 360 s ($d = 0.3$ m).

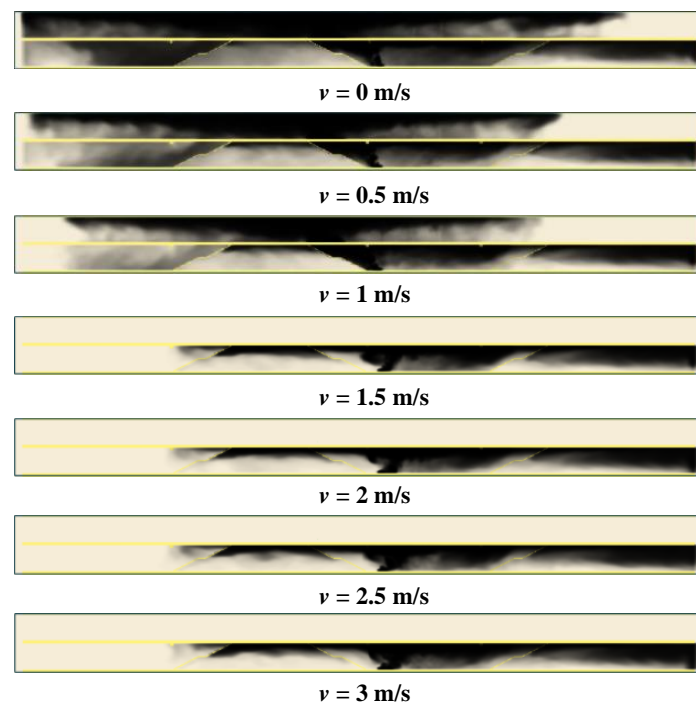


Figure 5. Smoke spread at 360 s ($d = 0.4$ m).

As shown in Figure 3 ($d = 0.2$ m), the smoke generated by the combustion of the fire source on the platform floor rises to the ceiling, forms a jet, spreads to both ends, and further spreads to the station hall through the stairs. It can be seen that, with the increase in the jet velocity of the air curtain, the smoke in the station hall is gradually decreasing, indicating that the air curtain plays a role in blocking smoke. However, the effect is not significant. Even at the maximum jet velocity set ($v = 3$ m/s), there is still a large amount of thick smoke in the station hall. Thus, all the set jet velocities cannot reach the level required to ensure the evacuation of passengers under this thickness.

As shown in Figure 4 ($d = 0.3$ m), with the increase in the jet velocity of the air curtain, the smoke-prevention performance is significantly improved. When the jet velocity reaches 1.5 m/s, there is almost no smoke in the station hall. When the jet velocity reaches more than 2 m/s, the smoke has been completely unable to spread to the station hall. As mentioned above, for the convenience of observation, the baffles on both sides of the stairs are hidden. Therefore, the smoke seen at the top of the stairs is actually smoke outside the baffle. At this point, there is a little smoke above the stairs. As shown in Figure 5, the situation is similar to Figure 4. It can be seen that when the jet velocity reaches 1.5 m/s, the smoke cannot spread to the station hall. It shows that the smoke is controlled on the platform and cannot spread to the station hall, which satisfies the requirements of passengers' evacuation. In addition, Figure 6 shows the velocity clouds for the different phases of the two cases where the air curtain worked and did not work. For Figure 6(1), it can be seen that the air curtain plays a role in the early stage of the fire, producing a deflecting effect on the flame, but as the heat release rate increased, the air curtain cannot effectively block the smoke, explained by the excessive lateral momentum of the smoke at this time, which broke through the prevention of the air curtain. Additionally, for Figure 6(2), it can be seen that it plays a role in different stages of the fire. The flames are deflected and maintained by the wind (even though the heat release rate increased to the maximum), which allow for the evacuation of the passengers on the stairs.

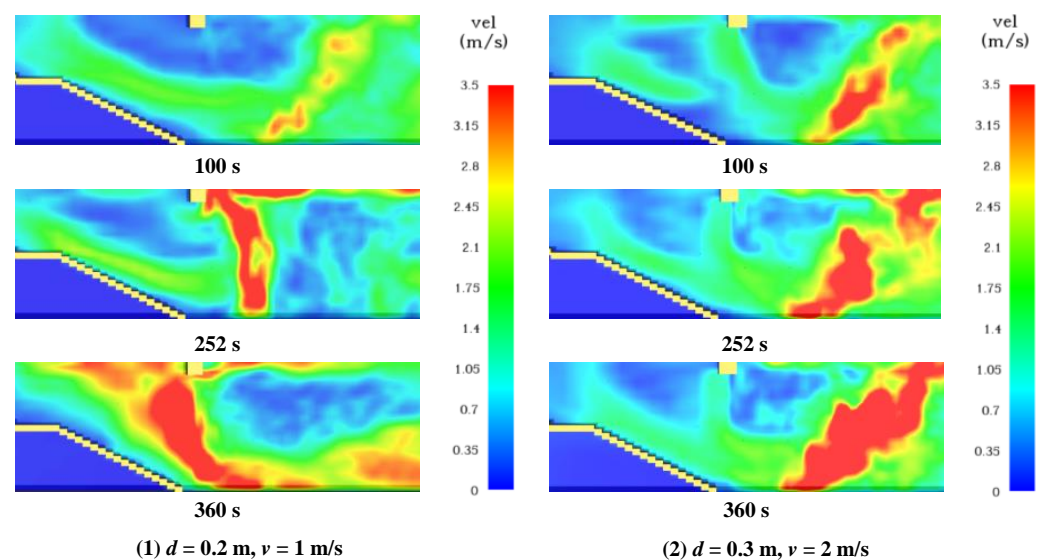


Figure 6. Smoke spread ($d = 0.2$ m, $v = 1$ m/s and $d = 0.3$ m, $v = 2$ m/s).

Therefore, under the condition of only positive pressure ventilation ($v = 0$ m/s), the positive pressure ventilation cannot completely ensure to prevent the smoke from spreading from the platform to the station hall. Only when the thickness of the air curtain reaches at least 0.3 m, and the jet velocity of the air curtain reaches at least 2 m/s, can the smoke-prevention performance of the air curtain be exerted.

3.1.2. Temperature

Figures 7–9, respectively, show the temperature changes over time at different jet velocities when the thickness of the air curtains is 0.2 m, 0.3 m, and 0.4 m.

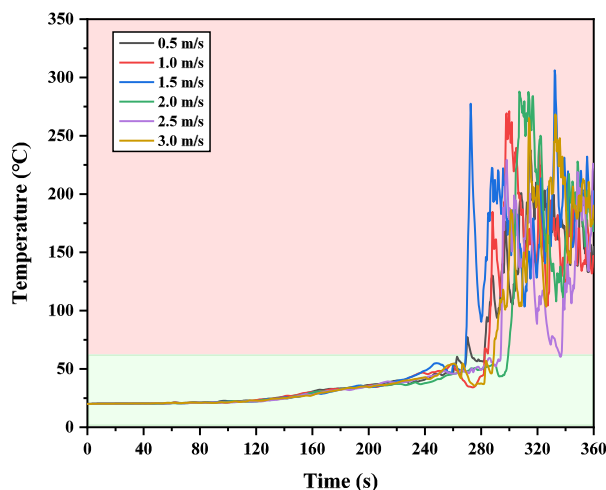


Figure 7. Temperature above the stairs at different jet velocities ($d = 0.2$ m).

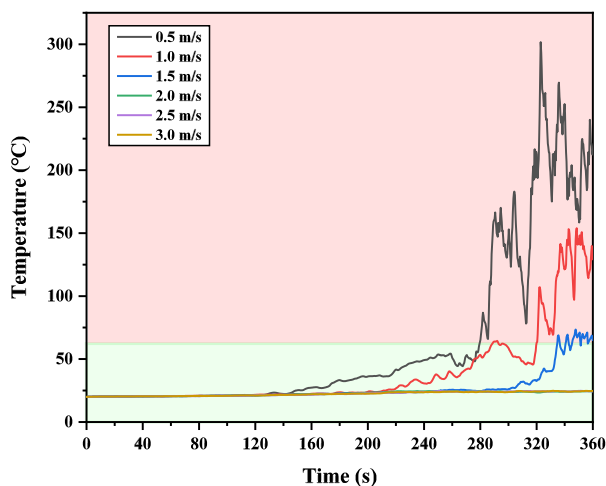


Figure 8. Temperature above the stairs at different jet velocities ($d = 0.3$ m).

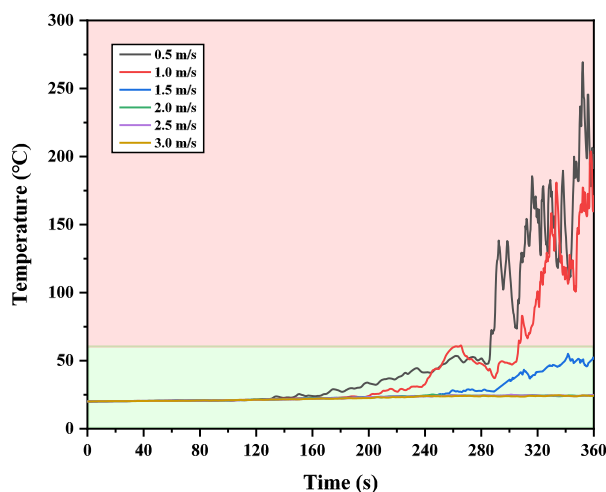


Figure 9. Temperature above the stairs at different jet velocities ($d = 0.4$ m).

Since the fire source adopts the model of t^2 fire, the temperature change is also similar to the power change of t^2 fire. In the early stage of the fire, the power of the fire source increases slowly, and the temperature also rises slowly. However, with the development of fire, the power of the fire increases rapidly in the later stage, which directly leads to a

sharp rise in temperature. As shown in Figure 7 ($d = 0.2$ m), due to the thin air curtain at this time, the smoke cannot be effectively blocked. A large amount of smoke breaks through the air curtain and spreads to the stairs, which leads to a rise in temperature above the stairs. None of the working conditions under this thickness can satisfy the evacuation requirements. As shown in Figure 8 ($d = 0.3$ m), the overall temperature is lower than that when $d = 0.2$ m. When the jet velocity is lower than 2 m/s, the temperature in the later stage of the fire is over 60 °C. This indicates that the smoke-prevention performance of the air curtain on the smoke is still not strong, and the smoke spreads to the stairs after breaking through the air curtain barriers, directly posing a threat to the human body. When the jet velocity reaches 2 m/s, the temperature above the stairs does not exceed 25 °C during the entire fire occurrence stage. This indicates that the air curtain effectively block the smoke and are conducive to the safe evacuation of passengers. As shown in Figure 9 ($d = 0.4$ m), the situation is similar to that when $d = 0.3$ m. At this time, it is worth noting that the temperature in the later stage at the jet velocity of 1.5 m/s reaches a maximum of 51 °C, which is lower than the given criterion of 60 °C. However, due to the increase in temperature, it proves that some of the smoke still breaks through the air curtain barriers and spreads to the stairs. Considering the decline in the endurance of the elderly and children, it may still cause harm to them. Luo et al. [31] conducted three sets of experiments by installing an air curtain with a size of $0.32 \text{ m} \times 0.1 \text{ m} \times 0.04 \text{ m}$ between the large space and the stairwell, and the power of the fire source was 0.2 kW. The temperature data shown in Figure 10 are similar to this paper's, and the smoke prevention effect of the air curtain was weak for a low air curtain velocity, which corresponds to condition 8 ($v = 0.5$ m/s) in Figure 8. However, as the velocity of the air curtains increases, the temperature of the stairwell shows a decreasing trend, but the larger the air curtain speed, the less obvious the decreasing trend, which corresponds to conditions 11–13 ($v = 2\text{--}3$ m/s) in Figure 8. The reason for the larger values of the air curtain parameters in this paper is that the heat release rate set in this paper is larger.

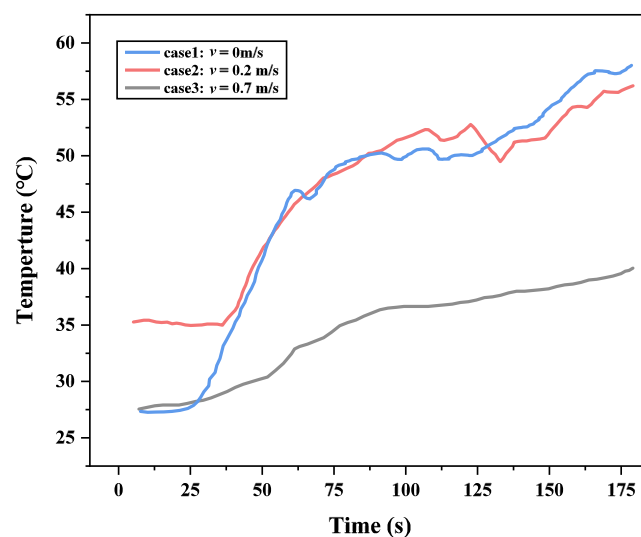


Figure 10. Experiments on stairwell temperature under air curtain protection from Luo et al.

Therefore, when the thickness of the air curtain reaches at least 0.3 m and the jet velocity reaches at least 2 m/s, the safe evacuation of passengers can be guaranteed.

3.1.3. Visibility

Figures 11–13, respectively, show visibility distribution at different jet velocities when the thickness of the air curtains is 0.2 m, 0.3 m, and 0.4 m.

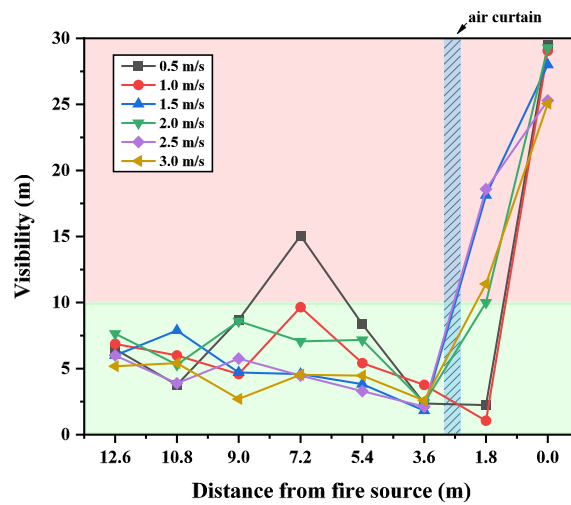


Figure 11. Visibility distribution on the left side of the fire source ($d = 0.2$ m).

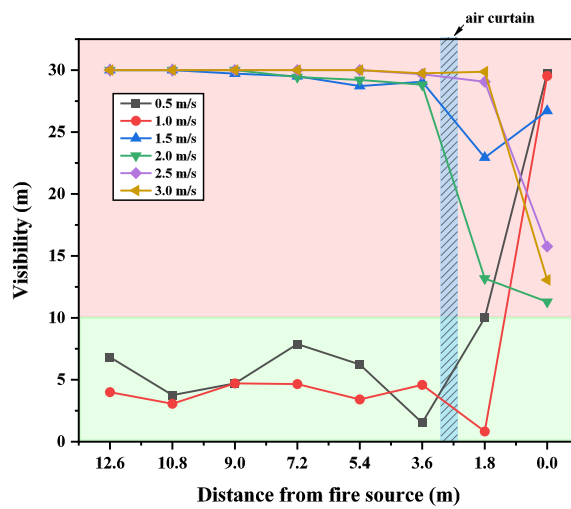


Figure 12. Visibility distribution on the left side of the fire source ($d = 0.3$ m).

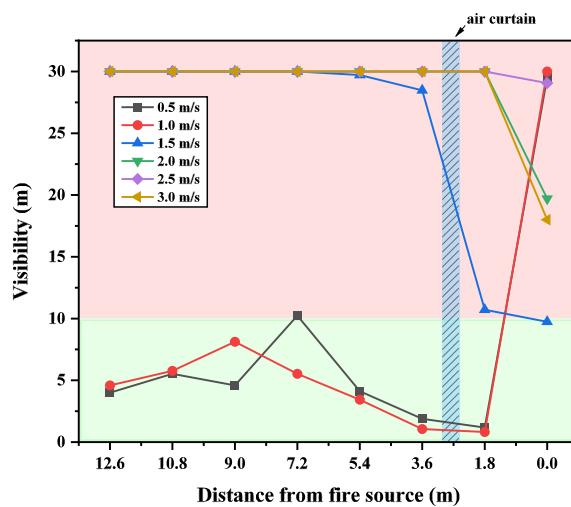


Figure 13. Visibility distribution on the left side of the fire source ($d = 0.4$ m).

As shown in Figure 11 ($d = 0.2$ m), the visibility at a height of 2 m above the stairs is almost always lower than 10 m, which is significantly lower than the visibility required under the criteria given above. As shown in Figure 12 ($d = 0.3$ m), it can be seen that when

the jet velocity is lower than 1.5 m/s, the visibility above the stairs is still less than 10 m, which threatens the safe evacuation of passengers. When the jet velocity is greater than or equal to 1.5 m/s, the visibility above the stairs exceeds 25 m, which is close to the visibility in normal conditions. As shown in Figure 13 ($d = 0.4$ m), the situation is similar to that when $d = 0.3$ m. When the jet velocity is greater than 1.5 m/s, the visibility above the stairs is stabilized at more than 25 m.

At the same time, it is found from Figures 11–13 that when the air curtain cannot work, the visibility on the left side of the air curtain is lower, and on the right side is higher. When the air curtain works, the result is reversed. The phenomenon can be explained by the fact that when $d = 0.2$ m, the air curtain is weak at this time and cannot effectively block the spread of fire smoke, and, due to the pressure difference caused by the temperature, a large amount of smoke with higher pressure spreads to the station hall with lower pressure through the stairs, causing the flames to tilt to the stairs. However, when $d \geq 0.3$ m, the air curtain is strong enough to cause the flame to tilt to the right, which prevents the smoke spreading to the station hall.

Therefore, only when the thickness of the air curtain reaches at least 0.3 m, and the jet velocity reaches at least 1.5 m/s, can the best visibility for people when escaping be achieved.

3.1.4. CO Concentration

Figures 14–16, respectively, show CO concentration changes over time at different jet velocities on the left side of the air curtain at a height of 2 m when the thickness of the air curtains is 0.2 m, 0.3 m, and 0.4 m.

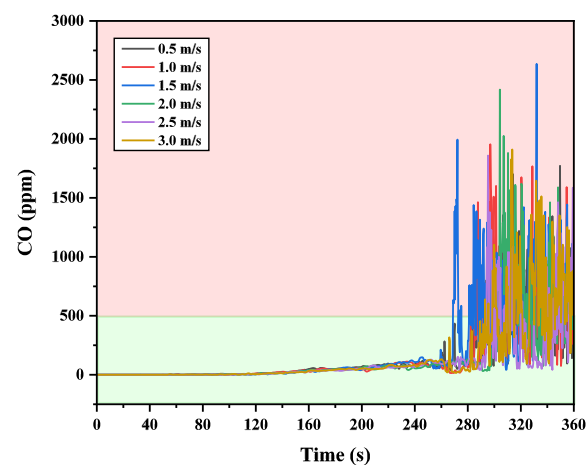


Figure 14. CO concentration above the stairs at different jet velocities ($d = 0.2$ m).

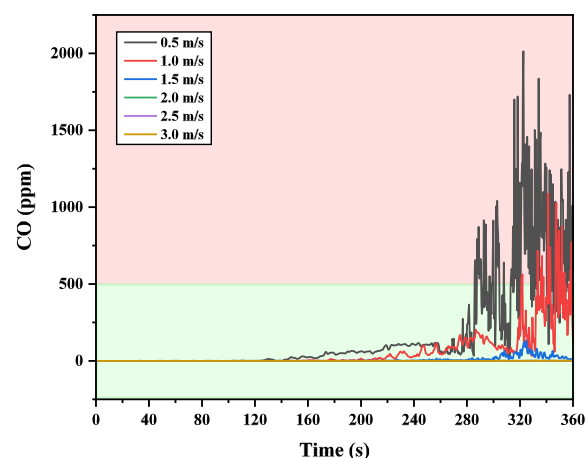


Figure 15. CO concentration above the stairs at different jet velocities ($d = 0.3$ m).

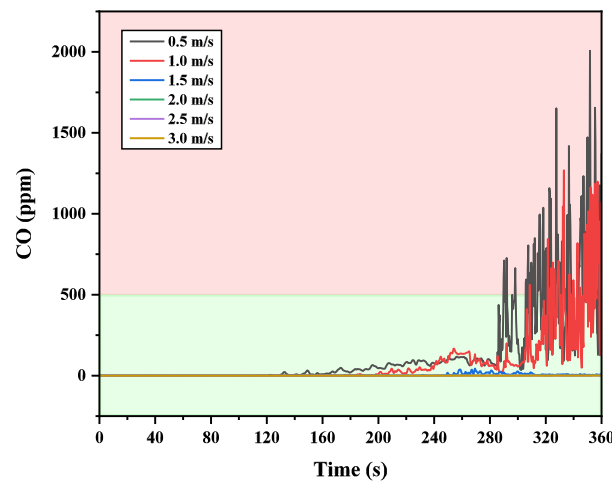


Figure 16. CO concentration above the stairs at different jet velocities ($d = 0.4$ m).

As shown in Figure 14 ($d = 0.2$ m), smoke can easily break through the thin air curtain. At the same time, due to the disturbance of the air curtains, the CO concentration under this thickness fluctuates greatly. However, it can be seen that the CO concentration begins to increase significantly after 260 s in all working conditions. At the same time, the value of the CO concentration is more than 500 ppm for most of the time thereafter, even reaching up to 2500 ppm. The results indicate that the air curtain under this thickness are not able to block smoke, and passengers are vulnerable to smoke poisoning in the fire. As shown in Figure 15 ($d = 0.3$ m), it can be seen that the CO concentration at the lower jet velocity ($v = 0.5$ m/s and $v = 1$ m/s) also increases significantly after 260 s. Although the fluctuation is also violent, it exceeds 500 ppm most of the time. After the jet velocity reaches 1.5 m/s, the CO concentration is controlled below 250 ppm. As shown in Figure 16 ($d = 0.4$ m), the situation is similar to that when the thickness of the air curtain is 0.3 m. After the jet velocity reaches 1.5 m/s, the maximum CO concentration cannot exceed 100 ppm. As shown in Figure 17(1), the average value of CO concentration under the effect of air curtain with different velocities was fitted by choosing the stable section after 300 s when $d = 0.3$ m. Hu et al. [15] conducted an experiment by lighting an oil pool fire in a rectangular space on one side. Additionally, the values of CO concentration behind the air curtain were examined. The variation of CO concentration versus the velocity of the air curtain was obtained, as shown in Figure 17(2). It can be seen that both have the same trend, and the CO concentration decreases very significantly as the velocity of air curtains increases and gradually tends to 0 ppm.

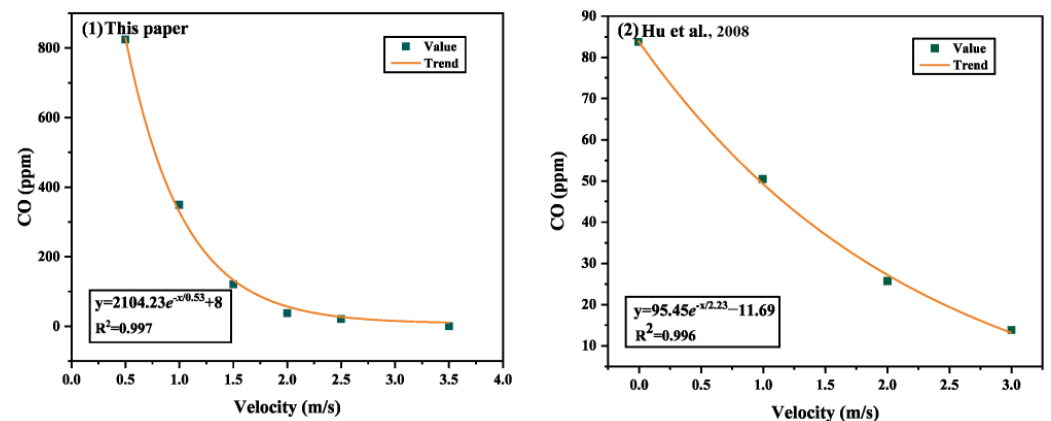


Figure 17. Comparison with changes in CO concentration of Hu et al. [15]. ($d = 0.3$ m).

Therefore, to prevent people from being poisoned by CO during the evacuation, the thickness of the air curtains shall be at least 0.3 m and the jet velocity shall be at least 1.5 m/s.

3.1.5. Sealing Effectiveness

Yu et al. determined the effectiveness of a vertical air curtain in blocking fire smoke in terms of the dimensionless number R of the pressure of the air curtain [32]:

$$R = \frac{I_a}{I_s} = \frac{\rho_a A_a v_a^2}{\rho_s A_s v_s^2} \tag{2}$$

where, ρ_a is the mean mass density of the air, kg/m^3 ; A_a is the cross-sectional area of the air curtain, m^2 ; v_a is the jet velocity of the air curtain, m/s ; ρ_s is the mean mass density of the layer flow underneath the ceiling over its depth, kg/m^3 ; A_s is the cross-sectional area of ceiling jet flow, m^2 ; v_s is the flow rate of the smoke, m/s .

Since only one fire source power is used in this paper, the momentum of the air curtain I_a will be used for evaluation. Table 3 shows I_a under various working conditions.

Table 3. I_a under various working conditions ($\text{kg}\cdot\text{m}\cdot\text{s}^{-2}$).

d (m)	v (m/s)							
	0.5	1	1.5	2	2.5	3	3.5	4
0.2	0.516	2.064	4.644	8.256	12.900	18.576	25.284	33.024
0.3	0.774	3.096	6.966	12.384	19.350	27.864	37.926	/
0.4	1.032	4.128	9.288	16.512	25.800	37.152	/	/

The performance of an air curtain in reducing heat and mass transfer is usually evaluated in terms of sealing effectiveness. The effectiveness $E_{sealing}$ is defined in terms of the difference between the overall temperature rise by Equation (3):

$$E_{sealing} = 1 - \frac{\Delta T}{\Delta T_{v=0}} \tag{3}$$

where, ΔT is the maximum temperature rise on the left side of the air curtain under various working conditions; $\Delta T_{v=0}$ is the maximum temperature rise at the same position without the air curtain.

Table 4 shows the sealing effectiveness under various working conditions. When $d \geq 0.3$ m and $v \geq 2$ m/s, the sealing effectiveness $E_{sealing}$ reached 98%. Similar to the previous findings, the air curtain at this point is a strong barrier against the high-temperature smoke generated by the fire. It was also found that, for the thin air curtain ($d = 0.2$ m), the sealing effectiveness showed a decrease at first with the increase in the jet velocity. The analysis of the phenomenon suggests that the thin air curtain has a limited sealing effectiveness, while a jet was formed by the air curtain on the floor that counteracts the smoke-prevention performance of positive pressure ventilation to a certain extent. However, when the velocity is large enough, the air curtain was able to compensate for the loss of the smoke-prevention function of positive pressure ventilation, so the sealing effectiveness is gradually enhanced.

Table 4. Sealing effectiveness under various working conditions (%).

d (m)	v (m/s)							
	0.5	1	1.5	2	2.5	3	3.5	4
0.2	27.336	16.326	4.617	10.690	30.219	23.895	26.002	28.669
0.3	9.970	55.355	82.191	98.420	98.407	98.400	98.367	/
0.4	16.896	38.719	89.200	98.277	98.323	98.473	/	/

Figure 18 illustrates the correspondence between sealing effectiveness and I_a . For different thicknesses of air curtains, the overall pattern is similar. The sealing effectiveness peaks when $I_a = 12.5 \text{ kg}\cdot\text{m}/\text{s}^2$. As the momentum of the air curtain increases, the sealing effectiveness is gradually enhanced. However, there is a critical value. Beyond this critical value, the sealing effectiveness will level off and the effect of increased momentum on the sealing effectiveness becomes slight. At this point, the increase in the thickness will have a greater impact on the sealing effectiveness.

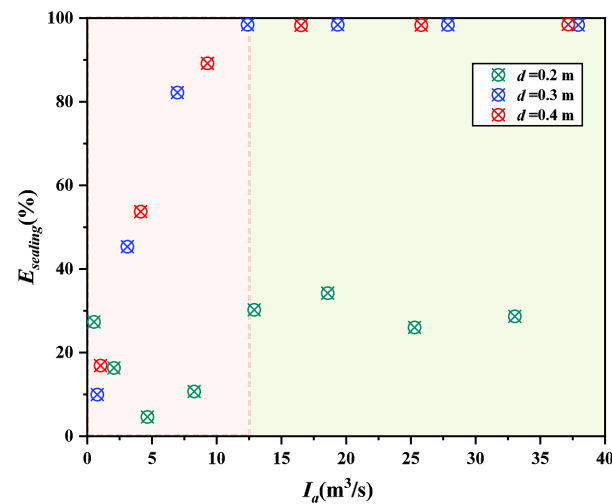


Figure 18. Sealing effectiveness $E_{sealing}$ at different I_a .

3.2. Comparison between with and without Positive Pressure Ventilation

3.2.1. Smoke Spread Process

Given the results of each working condition with the positive pressure ventilation, the thickness of the air curtains was selected to be 0.3 m and the jet velocity was selected to be 2 m/s to observe the smoke spread, temperature changes, visibility changes, and CO concentration changes without the positive pressure ventilation, and compare it with the condition with positive pressure ventilation.

Figure 19 shows the smoke spread in the subway station at 360 s in two cases. It can be seen that the situation without positive pressure ventilation is similar to that with positive pressure ventilation. There is less smoke on the platform due to the function of positive pressure ventilation. However, the difference is not obvious. Furthermore, the smoke is completely controlled on the platform. Figure 20 shows the temperature changes over time in two cases. In both cases the temperature reaches a maximum of 25°C and cannot exceed 60°C , maintaining a lower temperature level. It can be found that the temperature rises first and then stabilizes with time. The analysis suggests that the air curtain cannot completely cut off the heat transfer. Since the air curtain is close to the fire source, fresh air from the air curtain emitted from the top is heated due to encountering the hot plume and the close distance to the fire source. When it reaches the ground, a jet is formed, which then heats the air on the left side of the air curtain. Since the time to reach the maximum power set by the fire source is 252 s, the temperature also tends to be stable after 252 s, reaching a state of thermal equilibrium. Figure 21 shows the visibility distribution at different positions in two cases. It can be seen that the visibility on the left side of the air curtain is no different from the normal condition. It is maintained at a high level with a minimum of 27 m, which is greatly over the set criterion of 10 m. In this case, the line of sight of passengers is hardly affected. Figure 22 shows CO concentration changes over time in the two cases. Due to the strong smoke-prevention performance of the air curtain, and the location far from the ceiling, the CO concentration is very low. Given that the CO concentration is well below the criterion of 500 ppm, it can be ignored, and the toxic effect received during the evacuation of passengers will become very small.

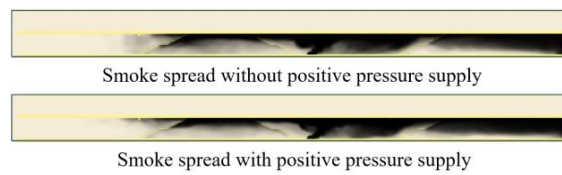


Figure 19. Smoke spread ($d = 0.3 \text{ m}$, $v = 2 \text{ m/s}$).

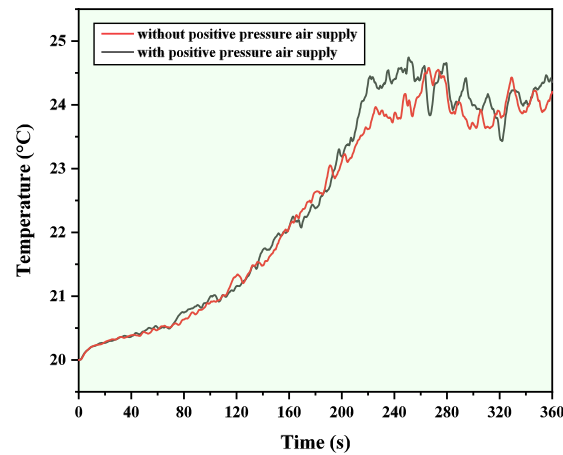


Figure 20. Temperature above the stairs ($d = 0.3 \text{ m}$, $v = 2 \text{ m/s}$).

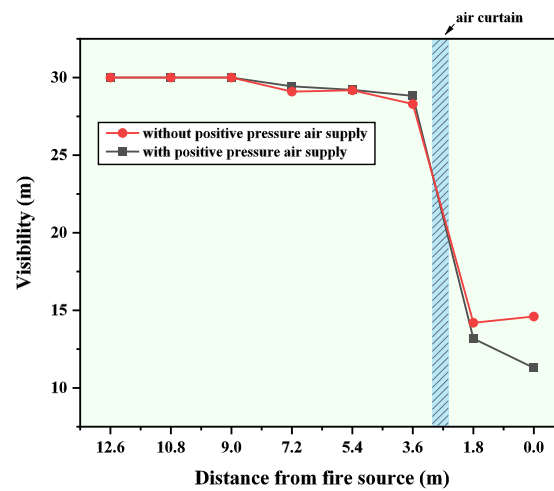


Figure 21. Visibility distribution on the left side of the fire source ($d = 0.3 \text{ m}$, $v = 2 \text{ m/s}$).

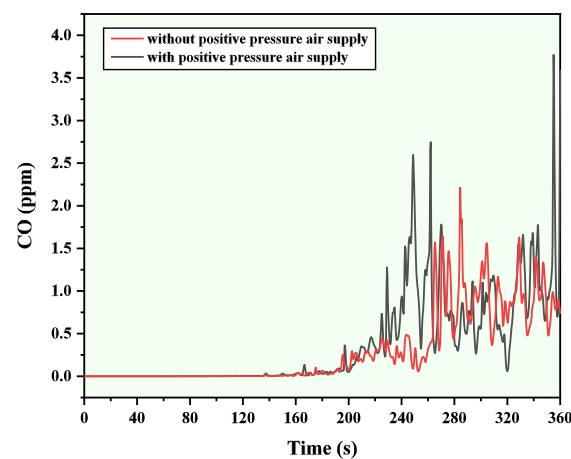


Figure 22. CO concentration above the stairs ($d = 0.3 \text{ m}$, $v = 2 \text{ m/s}$).

3.2.2. Energy-Saving Effectiveness of Air Curtain

To further quantify the energy-saving effect, the energy-saving efficiency E_{saving} is defined in Equation (4):

$$E_{saving} = 1 - \frac{Q_a}{Q_p} \quad (4)$$

where, Q_a is the volume flow rate of the air curtain when the air curtain is working, m^3/s ; Q_p is the volume flow rate of positive pressure ventilation, m^3/s .

For working condition $d = 0.3 \text{ m}$, $v = 2 \text{ m/s}$, the energy saving efficiency E_{saving} reaches 85.2%. This indicates that the air curtain is superior to positive pressure ventilation in smoke-prevention targeting and energy saving.

Therefore, by comparison, it can be concluded that various indicators under the conditions of positive pressure ventilation and no positive pressure ventilation are similar, and all were lower than the criteria given in this paper. The use of positive pressure ventilation to block smoke in subway stations means higher energy consumption. The application of air curtains can replace the effect of positive pressure ventilation in blocking the spread of smoke from the platform to the station hall.

4. Conclusions

The smoke-prevention performance of air curtains in the event of a 3 MW fire in a common island-type subway station was numerically studied using FDS. The performance was demonstrated from the four aspects of smoke spread, temperature, visibility, and CO concentration. This research will provide new ideas for the smoke-prevention systems of subway stations, and further improve the ability to ensure the safe evacuation of passengers. The main research conclusions are summarized as follows:

- (1) Compared with the subway station fire scene without air curtains, the installation of air curtains can block the spread of smoke from the platform to the station hall to a certain extent.
- (2) For lower thicknesses and velocities of the air curtains, it cannot work well to prevent the smoke. As the jet velocity reaches 2 m/s and the thickness reaches 0.3 m, the smoke is almost completely controlled at the platform. At this point, the time for the safe evacuation of passengers has been greatly extended.
- (3) The sealing effectiveness peaks when $I_a = 12.5 \text{ kg}\cdot\text{m}/\text{s}^2$. As the air curtain momentum increases, the sealing effectiveness is gradually enhanced. However, there is a critical value. Beyond this critical value, the sealing effectiveness will level off and the effect of the increase in the velocity on the sealing effectiveness will become slight. At this point, the increase in the thickness will have a greater impact.
- (4) For working condition 11 ($d = 0.3 \text{ m}$, $v = 2 \text{ m/s}$), an energy-saving efficiency of 85.2% can be achieved by replacing positive pressure ventilation with air curtains.

In the next step, we will further determine the mathematical relationship between air curtain momentum and the sealing effectiveness $E_{sealing}$ through experiments.

Author Contributions: Conceptualization, X.Y. and Y.Z.; methodology, Y.Z.; software, X.Y., validation, H.Y. and H.M.; formal analysis, Z.J.; investigation, X.Y.; resources, H.Y.; data curation, H.M. and Y.X.; writing—original draft preparation, X.Y.; writing—review and editing, X.Y. and Y.Z.; visualization, H.Y., H.M., Y.X. and Z.J.; supervision, Y.Z.; project administration, Y.Z.; funding acquisition, H.Y., H.M., Y.X. and Z.J. All authors have read and agreed to the published version of the manuscript.

Funding: This study is supported by the National Natural Science Foundation of China (No. 52278545), Natural Science Foundation of Hunan Province (No. 2021JJ30860), and the Fundamental Research Funds for the Central Universities of Central South University (No. 2023ZZTS0951).

Data Availability Statement: Data will be made available on request.

Conflicts of Interest: The authors declare no conflict of interest.

References

1. Wang, Q.; Jin, S.; Hou, Z. Cooperative MFAILC for Multiple Subway Trains With Actuator Faults and Actuator Saturation. *IEEE Trans. Veh. Technol.* **2022**, *71*, 8164–8174. [[CrossRef](#)]
2. Gao, R.; Li, A.; Zhang, Y.; Luo, N. How domes improve fire safety in subway stations. *Saf. Sci.* **2015**, *80*, 94–104. [[CrossRef](#)]
3. Shi, C.; Zhong, M.; Nong, X.; He, L.; Shi, J.; Feng, G. Modeling and safety strategy of passenger evacuation in a metro station in China. *Saf. Sci.* **2012**, *50*, 1319–1332. [[CrossRef](#)]
4. Carvel, R. Lessons learned from catastrophic fires in tunnels. *Proc. Inst. Civ. Eng.* **2008**, *161*, 49–53. [[CrossRef](#)]
5. Tsukahara, M.; Koshihara, Y.; Ohtani, H. Effectiveness of downward evacuation in a large-scale subway fire using Fire Dynamics Simulator. *Tunn. Undergr. Space Technol.* **2011**, *26*, 573–581. [[CrossRef](#)]
6. Hill, I.R. Immediate Causes of Death in Fires. *Med. Sci. Law.* **1989**, *29*, 287–292. [[CrossRef](#)] [[PubMed](#)]
7. GB/T 33668-2017; Code for Safety Evacuation of Metro. China National Standard: Beijing, China, 2017.
8. Zhou, Y.; Bu, R.; Gong, J.; Xu, Z.; Chen, H.; Fan, C. Numerical investigation on the effectiveness of positive pressure ventilation technology in a multi-layer subway station. *Indoor Built Environ.* **2019**, *28*, 984–998. [[CrossRef](#)]
9. Krajewski, G.; Węgrzyński, W. Air curtain as a barrier for smoke in case of fire: Numerical modelling. *Bull. Pol. Acad. Sci. Tech. Sci.* **2015**, *63*, 145–153. [[CrossRef](#)]
10. Yang, H.; Yuen, R.; Zhang, H.P. Numerical Study of Smoke Control for Underground Platform in a High-Speed Railway Station. *AMM* **2012**, 256–259, 2803–2812. [[CrossRef](#)]
11. Luo, N.; Li, A.; Gao, R.; Tian, Z.; Zhang, W.; Mei, S.; Feng, L.; Ma, P. An experiment and simulation of smoke confinement and exhaust efficiency utilizing a modified Opposite Double-Jet Air Curtain. *Saf. Sci.* **2013**, *55*, 17–25. [[CrossRef](#)]
12. Razeghi, S.M.J.; Safarzadeh, M.; Pasharshahi, H. Evaluation of air curtain and emergency exhaust system for smoke confinement of an enclosure. *J. Build. Eng.* **2021**, *33*, 101650. [[CrossRef](#)]
13. Gupta, S.; Pavageau, M.; Elicer-Cortés, J.-C. Cellular confinement of tunnel sections between two air curtains. *Build. Environ.* **2007**, *42*, 3352–3365. [[CrossRef](#)]
14. Zhou, Z.; Lu, Y.; Cui, Y. Study on the Effect of Jet Direction of Compound Air Curtain on Smoke Control. *Energies* **2021**, *14*, 6983. [[CrossRef](#)]
15. Hu, L.; Zhou, J.; Huo, R.; Peng, W.; Wang, H. Confinement of fire-induced smoke and carbon monoxide transportation by air curtain in channels. *J. Hazard. Mater.* **2008**, *156*, 327–334. [[CrossRef](#)]
16. Jung, U.-H.; Kim, S.; Yang, S.-H.; Kim, J.-H.; Choi, Y.-S. Numerical study of air curtain systems for blocking smoke in tunnel fires. *J. Mech. Sci. Technol.* **2016**, *30*, 4961–4969. [[CrossRef](#)]
17. Jin, X.; Gong, J.; Lin, Z.; Hua, S. The Influence of Air Curtains on Fire Smoke in Tunnels. *IJHT* **2022**, *40*, 569–576. [[CrossRef](#)]
18. Chen, Z.; Liu, Z.; Li, X.; Linqi, H.; Niu, G. Numerical study of the effect of air curtains on smoke blocking and leakage heat flux in tunnel fires. *Case Stud. Therm. Eng.* **2022**, *35*, 102164. [[CrossRef](#)]
19. Gao, D.; Li, T.; Mei, X.; Chen, Z.; You, S.; Wang, Z.; Wang, K.; Lin, P. Effectiveness of smoke confinement of air curtain in tunnel fire. *Fire Technol.* **2020**, *56*, 2283–2314. [[CrossRef](#)]
20. Du, F.; Zhang, Q.; Wang, K.; Cui, W.; Guo, Y.; Deng, Y. Study on crowd evacuation in subway transfer station fires based on numerical simulation. *Emerg. Manag. Sci. Technol.* **2022**, *2*, 16. [[CrossRef](#)]
21. Liu, Y.; Li, Y.Z.; Ingason, H.; Liu, F. Control of thermal-driven smoke flow at stairways in a subway platform fire. *Int. J. Therm. Sci.* **2021**, *165*, 106937. [[CrossRef](#)]
22. Hansell, G.; Morgan, H. *Design Approaches for Smoke Control in Atrium Buildings*; Fire Research Station Borehamwood: Borehamwood, UK, 1994.
23. NFPA 130; Standard for Fixed Guideway Transit and Passenger Rail Systems. National Fire Protection Association: Quincy, MA, USA, 2007.
24. Xiong, S.; Lv, W.; Xiong, X.; Liu, D.; Li, X.; Zhao, C. Research progress and application of emergency plans in China: A review. *Emerg. Manag. Sci. Technol.* **2023**, *3*, 3. [[CrossRef](#)]
25. Li, X.; Maghelal, P.; Arlikatti, S.; Dorsett, C. Review of evacuee mobilization challenges causing time-lag: Conceptualizing a new framework. *Emerg. Manag. Sci. Technol.* **2022**, *2*, 20. [[CrossRef](#)]
26. Shao, X.; Ye, R.; Wang, J.; Feng, J.; Wang, Y.; Jiang, J. Progress and prospects in crowd safety evacuation research in China. *Emerg. Manag. Sci. Technol.* **2023**, *3*, 1. [[CrossRef](#)]
27. Cai, T.; Wang, J.; Zhang, C.; Cao, M.; Jiang, S.; Wang, X.; Wang, B.; Hu, W.; Hu, Y. Halogen and halogen-free flame retarded biologically-based polyamide with markedly suppressed smoke and toxic gases releases. *Compos. Part B Eng.* **2020**, *184*, 107737. [[CrossRef](#)]
28. Liang, Q.; Li, Y.; Li, J.; Xu, H.; Li, K. Numerical studies on the smoke control by water mist screens with transverse ventilation in tunnel fires. *Tunn. Undergr. Space Technol.* **2017**, *64*, 177–183. [[CrossRef](#)]
29. Hurley, M.J.; Gottuk, D.T.; Hall, J.R., Jr.; Harada, K.; Kuligowski, E.D.; Puchovsky, M.; Watts, J.M., Jr.; Wieczorek, C.J. *SFPE Handbook of Fire Protection Engineering*; Springer: Berlin/Heidelberg, Germany, 2015.
30. Institution, B.S. *Application of Fire Safety Engineering Principles to the Design of Buildings*; British Standards Institution: Chiswick, UK, 2021.

31. Luo, N.; Li, A.; Gao, R.; Zhang, W.; Tian, Z. An experiment and simulation of smoke confinement utilizing an air curtain. *Saf. Sci.* **2013**, *59*, 10–18. [[CrossRef](#)]
32. Yu, L.-X.; Beji, T.; Zadeh, S.E.; Liu, F.; Merci, B. Simulations of Smoke Flow Fields in a Wind Tunnel Under the Effect of an Air Curtain for Smoke Confinement. *Fire Technol.* **2016**, *52*, 2007–2026. [[CrossRef](#)]

Disclaimer/Publisher’s Note: The statements, opinions and data contained in all publications are solely those of the individual author(s) and contributor(s) and not of MDPI and/or the editor(s). MDPI and/or the editor(s) disclaim responsibility for any injury to people or property resulting from any ideas, methods, instructions or products referred to in the content.